702255

ANL-7060

ANL-7060

Argonne National Laboratory

RADIOLOGICAL PHYSICS DIVISION

ANNUAL REPORT
JULY 1964 THROUGH JUNE 1965

REPOSITORY Argonne Lab
COLLECTION ER Division Annual Reports
BOX No.
FOLDER

PARTIAL DOCUMENT

0016508

TABLE OF CONTENTS

1 Further evidence for a hidden transition in biphenyl
I. B. BERLMAN and O. J. STEINGRABER

1 Mirror symmetry and spectra of aromatic molecules: Preliminary report
I. B. BERLMAN, F. HIRAYAMA, and M. INOKUTI

2 Scintillations and energy transfer in argon-nitrogen mixtures
HARVEY A. SCHULTZ

2 Ion-ion recombination rates in the gas phase
JAMES C. PERSON

2 Photoionization, excitation, and dissociation
JAMES C. PERSON

3 An isotope effect in the photoionization efficiency for benzene
JAMES C. PERSON

6 Comparison of an isotope effect in photoionization and in electron-impact ionization of molecules
JAMES C. PERSON

7 Influence of energy transfer by the exchange mechanism on donor luminescence
M. INOKUTI and F. HIRAYAMA

7 Some properties of the generalized oscillator strength and their relation to inelastic scattering of charged particles
M. INOKUTI and R. L. PLATZMAN

10 The latent period for radiation-induced osteosarcoma
PATRICIA M. FAILLA

12 Radiation response of rotifers exposed at different stages
PATRICIA M. FAILLA

15 LiF thermoluminescent dosimetry for beta rays
JACOB KASTNER, RAMESH HUKKOO, and B. G. OLTMAN

19 LiF thermoluminescent response to fast neutrons
JACOB KASTNER, B. G. OLTMAN and PETE TEDESCHI

22 LiF thermoluminescence for neutron image storage
JACOB KASTNER, HAROLD BERGER, and I. R. KRASKA

24 Modification of computer program 1977/RPY 146. Cosmic-ray neutron background (NEUTBAK)
JOSEPH H. KLEMS

25 A computer program, RPY 157X, to derive the cosmic-ray neutron background when multiple scattering in the detector is significant
JOSEPH H. KLEMS

33 Specific primary ionization in gases by high-energy electrons
F. F. RIEKE and W. PREPEJCHAL

37 The doses from Thorotrast and migrated descendants: status, prospects, and implications
L. D. MARINELLI

45 Preliminary analysis of a method for whole-body counting
P. J. BROCKWELL and L. D. MARINELLI

46 Computer program for assay of complex mixtures of gamma-emitting radionuclides
HENRY F. LUCAS, JR.

50 Measurements of water vapor, radon concentration, and differential pressure in the air system to the underground counting facility
RICHARD B. HOLTZMAN and HENRY F. LUCAS, JR.

0016509

56 The Mössbauer effect from bone crystal surfaces
J. H. Marshall

59 Mössbauer effect in Cs^{133}
G. J. Perlow, A. J. F. Boyle, J. H. Marshall and S. L. Ruby

61 Concentration of radium and strontium in bone, blood, and soft tissue in relation to calcium
Elizabeth Lloyd, J. H. Marshall, R. E. Rowland, and H. F. Lucas, Jr.

64 Studies on bone-seeking radioisotopes
Robert E. Rowland

69 Resorption and bone physiology
Robert E. Rowland

70 The retention of Ba^{133} in beagles
J. E. Farnham and R. E. Rowland

73 Thorium and uranium in the natural environment: a review of present knowledge
David N. Edgington

77 The estimation of thorium and uranium at the submicrogram level in bone
David N. Edgington

81 Strontium retention in mice treated with thyroid hormones
David J. Simmons and Patricia M. Failla

90 Autoradiographic investigation of collagen formation and endochondral ossification in mice and the effect of estrogen
David J. Simmons

93 A preliminary study of gamma rays emitted by Thorotrast patients: a) estimate of effective depth of liver in phantom; b) estimate of gamma-ray activity in the lower leg
H. A. May and L. D. Marinelli

99 Gamma-ray backgrounds in the RPY vault: stability and radon dependence
J. B. Corcoran and F. Markun

112 Multichannel analyzer data processing
J. B. Corcoran

113 A multitube preamplifier system
J. B. Corcoran, Dale Suddeth, and O. J. Steingraber

116 Radar detection of an ionized column in the lower atmosphere
Harry Moses, S. L. Halverson, Jacob Kastner, T. V. Banfield, G. E. Stout, and E. A. Mueller

120 Radon-222 concentration-height-time relationships
Harry Moses and J. E. Pearson

128 Meteorological instruments for air pollution surveys
G. Gill, N. Islitzer, T. Lemmons, D. Mazzarella, Harry Moses, and J. E. Pearson

128 The contribution of plants to atmospheric radon-222
J. E. Pearson and R. R. Dedolph

130 Determination of the vertical heat flux in the atmosphere by variance reduction analysis
Paul Frenzen

134 Instrumentation for atmospheric turbulence studies
Paul Frenzen

136 Publications

0016510

following estrogen treatment, it is probable that the endosteal reaction does not reflect a change in the gross nutritional status of the bone.

Because it is well known that estrogen treatment impedes both cartilage cell mitosis and mucopolysaccharide formation,[14] it would be reasonable to assume that the hormone exerted its primary action on some regulatory cell organelle. Recently, the electronmicrographic studies of Silberberg *et al.*[15] demonstrated hypertrophy of the Golgi zone and accelerated organelle development in articular cartilage cells of mice as early as 2 hours after hormone treatment. These changes, which were maximum after 16 hours, were related to a disturbance of carbohydrate synthesis by these chondrocytes, i.e., decreased production of mucopolysaccharides, and delayed endochondral ossification. In the present study, the radioproline marker demonstrated that estrogen had suppressed endochondral ossification (longitudinal bone growth) 24 hours after treatment.

SUMMARY

The effect of estrogen on the rate of collagen synthesis and new bone formation in the mouse was investigated by high resolution autoradiographic methods. H^3-proline and H^3-glycine were administered on the first and seventh days, respectively, following estrogen treatment, and the mice were sacrificed at various intervals during the 24 hours following each tracer injection. The position of the radioproline label on metaphyseal trabeculae indicated that the control bones grew in length 135 μ/day, whereas the bones from mice injected with estrogen 24 hours previously grew only 66 μ/day. Grain counts indicated that (a) the uptake of the labeled amino acids by osteoblasts, and (b) the subsequent transfer of the label with time after injection to surfaces of newly forming metaphyseal and endosteal bone was not affected by prior estrogen treatment. Silver grains were observed over the bone 16–24 hours after tracer administration. It was concluded that estrogen stimulates only the processes which promote the differentiation of osteoblasts in the bones of mice, and that the hormone has no effect on the functional capacity of individual osteoblasts to synthesize and form collagen.

REFERENCES

1. W. U. Gardner and C. A. Pfeiffer. *Proc. Soc. Exptl. Biol. Med.* **37**, 678 (1938).
2. M. R. Urist, A. M. Budy, and F. C. McLean. *Proc. Soc. Exptl. Med.* **68**, 324 (1948).
3. G. M. Vaes and G. Nichols, Jr. *Endocrinol.* **70**, 890 (1962).
4. D. J. Simmons. *Clin. Orthoped.* 1963, No. 26, 176.
5. B. Messier and C. P. Leblond. *Proc. Soc. Exptl. Biol. Med.* **96**, 7 (1957).
6. E. A. Tonna. *J. Gerontol.* **19**, 198 (1964).
7. D. J. Simmons and G. Nichols, Jr. *Am. J. Physiol.* In press, 1965.
8. J. E. Eastoe. *The Biochemistry and Physiology of Bone*, ed. G. H. Bourne. Academic Press, New York, 1956, p. 81.
9. M. R. Stetten. *Amino Acid Metabolism*, ed. W. McElroy and G. Glass. The Johns Hopkins Press, Baltimore, Md., 1955, p. 277.
10. E. A. Tonna, E. P. Cronkite, and M. Pavalec. *J. Histochem. Cytochem.* **11**, 720 (1963).
11. M. R. Urist, A. M. Budy, and F. C. McLean. *J. Bone Joint Surg.*, **32A**, 143 (1950).
12. L. W. Gorham and W. T. West. *Arch. Path.* **78**, 673 (1964).
13. M. Brookes and E. G. Lloyd. *J. Anat.* **95**, 220 (1961).
14. M. Silberberg and R. Silberberg. *Am. J. Anat.* **69**, 295 (1941).
15. R. Silberberg, M. Hasler, and M. Silberberg. *Am. J. Path.* **46**, 289 (1965).

A PRELIMINARY STUDY OF GAMMA RAYS EMITTED BY THOROTRAST PATIENTS:

a) Estimate of Effective Depth of Liver in Phantom

b) Estimate of Gamma Ray Activity in the Lower Leg

H. A. May and L. D. Marinelli

INTRODUCTION

Four individuals who received injections of colloidal Th^{232} and Th^{228} (Thorotrast) approximately 15 years ago have been examined in the whole-body counter. Initial injections for X-ray visualization of blood vessels of the cranial cavity were made at the Department of Radiology of a midwestern medical school. The evaluation of present body burden of these patients was undertaken in cooperation with that institution, in order to evaluate the cost and feasibility of a full-scale epidemiological study.

SCOPE AND METHODS

The primary purpose of this investigation is to evaluate the relationship between radiation dose and biological damage over long periods of time. In this case, the organs receiving the greatest exposure are the liver and spleen, with lesser amounts being received by lymph

0016511

nodes, kidneys, bone marrow and (in cases of significant extravasation) injection site tissue. An accurate assessment of accumulated dose requires quantitative knowledge of the local metabolic behaviour of each of the radioactive daughter products during the initial period following injection as well as the steady-state or equilibrium distribution.

Direct gamma spectrometry of the whole body may contribute to an understanding of this latter period by contributing the following information:

(1) Total body burden of Ac^{228} (MsTh 2), Pb^{212} (Th B), Bi^{212} (Th C), and Tl^{208} (Th C″).

(2) Lack of secular equilibrium between γ-ray emitters in the chain, presumably due to loss by recoil from the colloidal particle, with subsequent transport and elimination by normal body processes.

(3) Extent of deposition within the skeleton (primarily, within the red bone marrow), or within a specific portion of same.[1]

(4) Further information on the relative distribution of activity among the vital organs or other soft tissues. Although the problems of scanning and directional detection at the γ-ray energies concerned appear difficult and have not been entirely resolved (*vide infra*), such effort should contribute results which are not otherwise available to direct experimental approach.

In this study, two large NaI crystals have been used simultaneously, maintained in a fixed position relative to the patient for the duration of each count. Pulses from each are fed to individual multichannel analyzers.

The first count is made with an 11.5″ diameter by 4″ thick crystal suspended over the patient, at a distance of 1 meter from the lower surface of the crystal to the supporting "bed". Since counts are made with the patient prone and supine, a flat bed is preferred, although if curved into an arc of 1-meter radius, a slightly more uniform response to activity along the length of the patient is obtained. However, since 90 to 95% of the activity is believed to be in the liver and spleen, the arc offers no overwhelming advantage.

The second count is obtained after lowering the crystal until it almost touches the patient; by this means a certain degree of discrimination may be obtained between gamma rays originating in the abdomen and the extremities. However, as the spectrum extends to 2.615 MeV, additional discrimination by means of collimation would involve great bulk and weight. A crystal-to-bed distance of 35 cm has been adopted as standard, although an occasional obese individual may necessitate a greater separation. A second crystal, 7″ diameter by 3.5″ thick, facing upward, is located beneath the bed, with a spacing of 2.5 cm from its upper surface. The spectra from both crystals are accumulated simultaneously.*

Although the detection sensitivity is much greater at this spacing, it is also far more dependent upon the source volume and location within the body, and upon the amount of scattering and absorption from surrounding tissues. Can this limitation be overcome by making use of all the information contained in spectra from two detectors at a fixed separation? As a particularly simple possibility, the *in vivo* ratio of counting rates from the two detectors observed in a selected energy band might be utilized to give an indication of the "effective depth" of the source within the body, by reference to suitable phantom calibrations. Substantial independence of this ratio throughout the energy range would facilitate the estimate of depth. From a knowledge of the effective depth, an independent self-absorption correction of the total activity present may be made. Preliminary tests, in which point sources of ThO_2 in a 16-cm thick Presdwood phantom were used to calculate the position and activity of a phantom liver, gave results having acceptable accuracy.† (See Appendix I.)

COINCIDENCE TECHNIQUES

The decay scheme of Ac^{228} exhibits a number of cascade gamma rays, the principal pairs, with their relative intensities being[2]

278 keV	and	790 keV	(3)
328 keV		790 keV	(3)
408 keV		960 keV	(2)
460 keV		980 keV	(2.1)
460 keV		966 keV	(1.3)

In the decay of Tl^{208}, all lower-energy gamma rays are in coincidence with the 2.615-MeV line. The most intense of these are:

277 keV	(1)
511 keV	(25)
583 keV	(87)
860 keV	(12)

Thus it appears that operating the two detectors in

* Although two 11.5″ x 4″ crystals spaced symmetrically above and below the patient's midplane offer statistical advantages, budgetary limitations restricted us to the much less efficient procedures described here.

† Usefulness of the method in the present application appears to rest upon the accuracy with which these results can be extended to phantoms having a range of thickness compatible with that of the bodies they simulate. Likewise, the effect of variations among individual patients in size, shape, and location of the liver and spleen must be considered and evaluated. Computer matching and stripping of standard spectra by means of least squares techniques also appear to offer great possibilities and are under investigation.

0016512

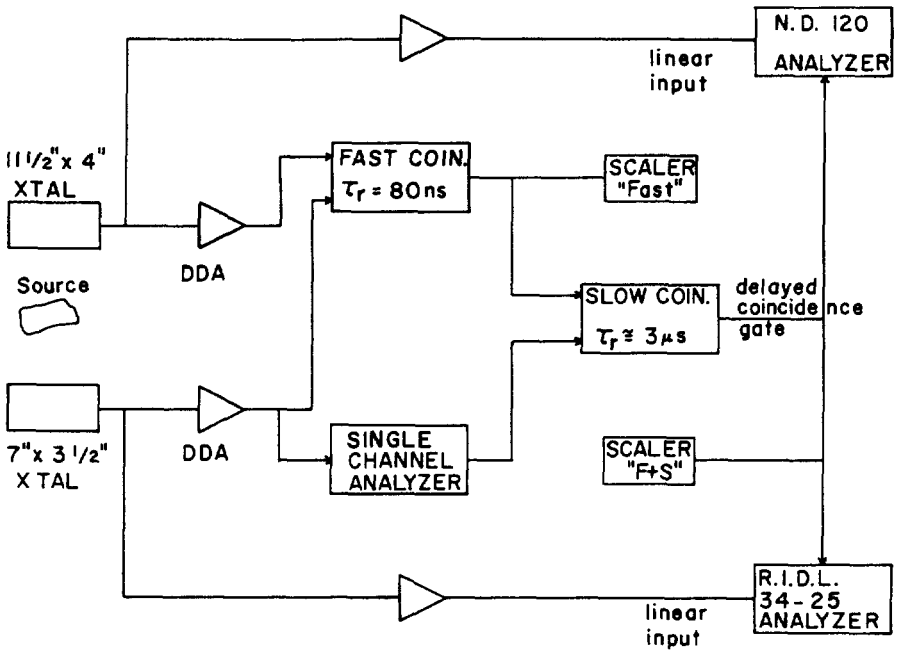

FIG. 43. Block diagram: electronic circuitry in fast-slow coincidence.

coincidence may lead to less complex spectra and a resulting ease of interpretation. By gating only on pulses of 1.6 MeV or more, response is completely limited to the gamma rays of Tl^{208}. At lower gating energies, both Ac^{228} and Tl^{208} contribute to the spectrum, and by a judicious choice of the energy band employed for gating, response to Ac^{228} may be maximized. From such coincidence spectra, the determination of the *relative* amounts of the two daughters is considerably simplified.

We have demonstrated that coincidence rates from typical Thorotrast patients in the geometry described above permit accumulation of statistically-significant data in counting periods of forty to sixty minutes. The electronic connections employed are indicated in the block diagram of Figure 43. Gating requirements are established by a conventional fast-slow coincidence system.[3] Pulses from both detectors are double-delay-line shaped and fed to zero-crossing detectors. A fast coincidence resolving time of roughly 80 nanoseconds is used. By carefully equalizing delays, much shorter times may be used without significantly reducing the real coincidence rate. However, chance coincidence background is always negligible, and this resolving time adequately allows for less-than-optimum delay adjustments, or minor gain changes. Pulses from the 7″ x 3.5″ crystal are energy-selected and, after slow coincidence, are employed to gate the analyzer which stores pulses from the large detector. The same gate supplied to the second analyzer serves to monitor the energy band selected by the single-channel analyzer and is only necessary during initial adjustment. We have found the single-channel analyzer to be remarkably stable over periods of months, during which it has been repeatedly turned off when not in use. Simultaneous recording of both the straight and coincidence spectra, or of two spectra gated by different energy regions, would undoubtedly make better use of the counting time. We have not yet tried this, largely from a desire to keep all of the data from each detector associated with its own analyzer. Results obtained so far suggest that the coincident rate depends upon source-to-detector orientation much more strongly than in the noncoincidence mode. Analysis of these data, together with phantom measurements to determine the dependence upon patient size and isotope distribution, is incomplete; hence, interpretation of the results must be deferred.

Evaluation of the skeletal burden located primarily, but not entirely, in the marrow, is also desired. Since the principal marrow sites, i.e., the sternum, vertebrae, and pelvic crests, are located in rather close proximity to the much more active deposits in liver and spleen, direct counting is out of the question. A method of detecting the lesser amounts of activity within the tibia and fibula has been investigated. The geometry employed is illustrated in Figure 44. Sensitivity to gamma rays from the soft tissue deposits is greatly reduced by coincidence requirements* and by a relatively modest amount of shielding below the patient's knees. With the

* In this case, as is well known, the counting rate is proportional to the product of the solid angles subtended by the source at the two detectors.

0016513

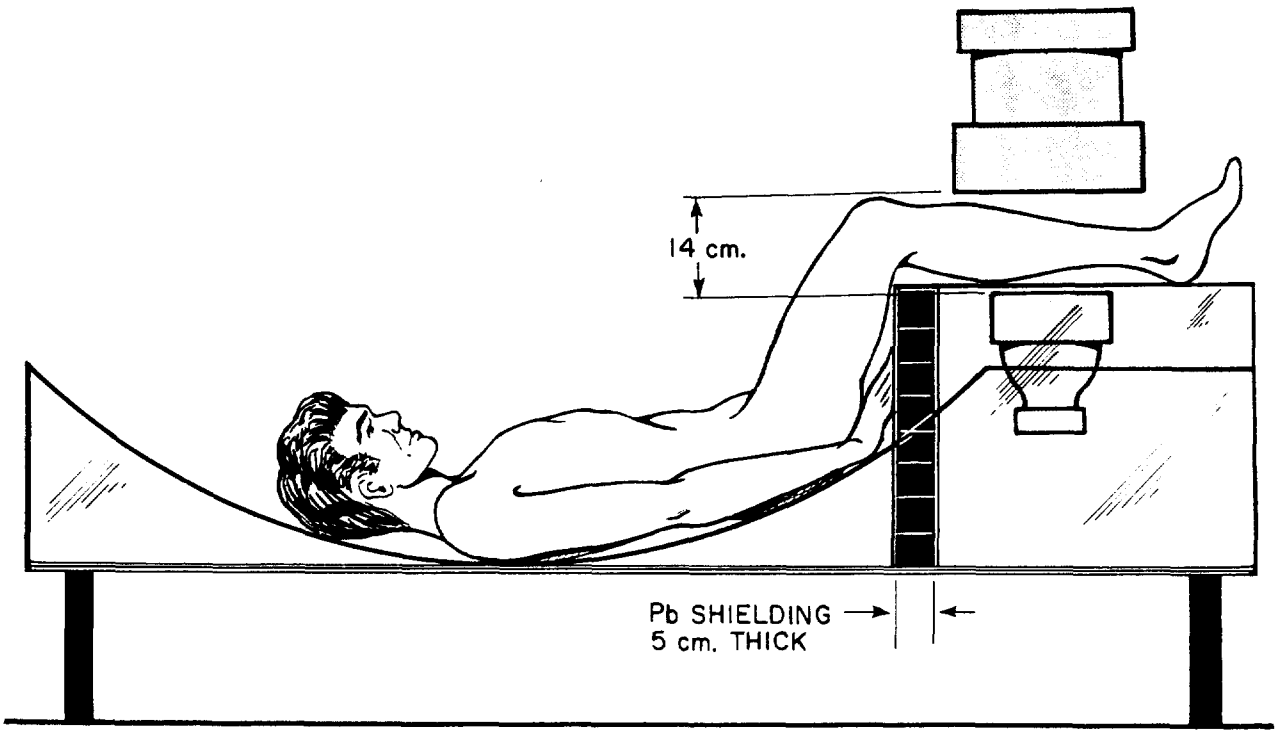

FIG. 44. Relative position of patient, detectors and shielding, as employed for leg counting.

two crystal faces spaced 14 cm apart, centered roughly between the distal surface of the patella and the external malleolus and with 5 cm of lead shielding as indicated, the following background counting rates are typically recorded by the upper crystal:*

(a) no patient, 14 cpm
(b) with thorium-free patient, 15 cpm
(c) as in (b) plus 25-cc bottle of Thorotrast placed alternately at the lower tip of the sternum and small of the back, to simulate a typical deposit within the soft tissues only, 16.5 cpm.

RESULTS

Data from the 11.5″ x 4″ crystal were accumulated on a 512-channel Nuclear Data analyzer, those from the 7″ x 3.5″ on a 400-channel RIDL instrument. Data output were punched on paper tape which was processed initially with a CDC 160A computer. For some processing requiring greater core memory capacity (spectrum normalization and fitting, digital plotting via Cal Comp plotter, etc.), the data are transferred via magnetic tape to the CDC 3600.

The raw data from Thorotrast patients have been corrected for estimated potassium and cesium burdens by subtraction of the spectrum obtained from a Thorotrast-free individual of comparable height and weight. Table 32 lists net counting rates observed in selected energy bands for the four patients studied. Typical backgrounds are also included. Estimates of activity in the lower leg and feet are given in Appendix II.

Special thanks are due to Dr. W. B. Swanson and Dr. F. J. Hodges of the University Medical Center in Ann Arbor, Michigan for making the patients available for this study and supplying essential information relevant to this investigation. Mr. Paul Hess contributed to the design and construction of phantoms and in the taking and reduction of data.

APPENDIX I

INTRODUCTION

A method of correcting whole-body counting data for the effects of self-absorption loss has been investigated, which is applicable when it is known *a priori* that the activity to be measured is concentrated in a specific region or organ. The immediate application to the case of liver deposits in Thorotrast-injected patients has already been mentioned, and the discussion will deal with techniques adapted to this specific end, although the general method is believed to have greater usefulness.

It is desired to determine the amount of gamma-emitting element located in an organ whose position within the body, and whose size and shape, are known only roughly. Two crystal detectors are employed, lo-

* In the energy region 200 keV-2.8 MeV, and in coincidence with gamma rays detected by the lower crystal between 485 keV and 2.92 MeV.

0016514

cated on opposite sides of the body and separated by a fixed distance, so positioned that the line joining them and coinciding with their axes also intersects the center of the region of interest. The two detectors should subtend nearly equal solid angles.

On the basis of preliminary measurements, it appears that the *ratio* of counting rates in the two detectors, in a given energy band, uniquely determines the location of an effective "center of activity" of the unknown source along the axis as established above. The location, i.e., the distance from either detector (or any other fixed reference point) to the center of activity may be evaluated by reference to calibration data obtained with a suitable phantom, in which the location of a point source of the same radionuclide is systematically varied. Since the intensity of the calibrating source may also be known with precision, the same calibration may be used to estimate the amount of activity present in the unknown.

EXPERIMENTAL PROCEDURE

The point source employed was a 25-cc glass bottle of the type used for packaging Thorotrast. It has been observed that the dextrin buffering of the colloidal Thorotrast fails after extended storage time, permitting clumping of the material and consequent nonuniform distribution within the bottle; therefore, a measured amount of ThO_2 powder was uniformly distributed within the source bottle in agar medium. The phantom consisted of $^1/_4''$ thick Presdwood sheets, 20 x 24 cm in size. Twenty-five of these provided a phantom thickness of 16 cm. Counts from both detectors at a separation of 37 cm were accumulated for 20 min at each of 15 source locations, spanning the entire range of phantom thickness. A plot of R_i versus position in the phantom was obtained, where R_i is the ratio of counting rate in the 11.5″ x 4″ crystal to that in the 7″ x 3.5″ crystal, in the i th energy band. The five energy regions employed were those of Table 32, namely:

i = 1, 200–430 keV
2, 430–700 keV
3, 0.83–1.10 MeV
4, 1.45–1.75 MeV
5, 2.4–2.8 MeV.

R values were observed ranging from about 3.0 at a distance of 2.5 cm below the upper surface of the phantom (19 cm from the face of the 11.5″ x 4″ crystal) to 0.25 at the other extreme of the phantom, 13.5 cm below the upper surface. A small but consistent variation of the ratio with energy was observed at fixed source position.

The unknown employed was a ThO_2-loaded "liver" molded of Mix D[4]—a paraffin-polyethylene mixture

TABLE 32. NET COUNTING RATES OBSERVED IN SELECTED ENERGY BANDS FOR THE FOUR PATIENTS STUDIED

Patient	Weight (lbs)	Height	Age (yrs)	Date injected	Amt. injected (cc)
JJ	185	5′10″	43	1949	30
MM	105	5′	62	1949	28 (?)
RP	180	5′10	49	1949	30
HR	186	5′11″	62	1952	60

Patient	Net counting rate (cpm)					
	Energy band					
	200 – 430 keV	430 – 700 keV	0.830 – 1.1 MeV	1.45 – 1.75 MeV	2.4 – 2.8 MeV	Total
At 1 meter, 11½″ x 4″ crystal						
JJ[a]	7,074	948	567	130	172	19,158
MM	1,465	621	379	65	116	5,680
RP	1,255	507	306	80	96	4,351
HR	4,680	1,957	1,134	242	358	16,332
Bkgnd[b]	568	362	127	113	24	2,114
At 35 cm, 11½″ x 4″ crystal						
JJ	41,426	6,274	4,056	1,082	1,182	118,830
MM	10,200	4,527	3,051	597	829	38,582
RP	10,472	4,747	2,920	660	861	37,405
HR	30,350	13,356	8,063	1,740	2,476	108,500
Bkgnd	1,005	781	190	223	24	3,700
At 10 cm, 7″ x 3½″ crystal (under table)						
JJ[a]	33,150	3,430	1,977	432	477	104,460
MM	6,911	2,908	1,797	354	359	25,494
RP	4,227	1,823	1,034	234	258	16,992
HR	13,770	6,039	3,108	736	904	54,847
Bkgnd	391	295	76	44	5.4	1,620
At 35 cm, 11½″ x 4″ crystal in coincidence						
JJ	42.7	20.6	4.95	1.5	6.5	104
MM	62	44	5.8	1.5	8.9	135
RP	33	28	4.2	0.75	4.8	79
HR	97	81	12	4.0	13	229
Bkgnd	2.2	2.5	1	0.5	0.4	8
In special "shin-counting" geometry, 11½″ x 4″ crystal in coincidence						
JJ	8.7	10	1.4	0.6	2.1	25.3
MM	7.1	7.2	0.8	0.6	1.7	20
RP	5.1	5.8	0.55	0	1.5	14.3
HR	14.0	12.6	1.6	0.6	2.8	35.5
Bkgnd	3.7	4.05	1.5	0.77	0.58	15.0

[a] Patient had received ≈1 mCi Hg^{197} for brain scan approximately 4 months previous to count. The numbers in Cols. 1 and 6 reflect the residual burden, apparently concentrated in kidneys.

[b] All the background data in Table 32 were obtained by counting an average adult, and thus include a normal, or typical, contribution from K^{40} and Cs^{137}.

0016515

TABLE 33. SUMMARY OF RESULTS ON SMALL (850 G) LIVER CONTAINING 0.98 G ThO_2

Depth to center line of paraffin	5.1	8.0	11.1
Mean ratio (net cpm [11.5 × 4]/ net cpm [7 × 3.5])	2.73	1.54	0.739
Calculated "point equivalent depth" (cm)	3.83 ± 0.06	6.8 ± 0.1	9.2 ± 0.2
Difference, geometrical center line to "point equivalet depth" (cm)	1.3	1.2	1.9
Calculated activity ThO_2 (g)	0.929 ± 0.011	0.93 ± 0.02	0.894 ± 0.04

All errors are one standard deviation.

with small quantities of magnesium and titanium oxides added to match more nearly the effective Z of water or tissue. It has been shown[5] that this material is very closely water-equivalent in the energy range of interest. The "liver" dimensions were roughly 21 x 17 x 7 cm; its mass of 850 g was somewhat less than that of a normal adult male. An outer layer of epoxy plastic approximately 1 mm in thickness was applied to avoid surface damage and loss of radioactivity, and it was then embedded in a rectangular block of plain paraffin in order to facilitate reproducible positioning within the Presdwood phantom. Additional Presdwood sheets having a large rectangular cut-out to accommodate the paraffin block were utilized.

Data were taken with the "unknown liver," containing 0.98 g ThO_2, at three depths within the phantom. All numbers were corrected for background, and the net counting-rate ratios converted to "effective point-equivalent depths." These calculated depths, which are remarkably consistent over the range of energies employed, differ from the reference distance as measured to the midplane by a nearly constant amount. The activity of the unknown was then calculated from the observed counting rate of the reference point source when located at the same depth. In practice, linear interpolation from the nearest calibration depths was employed to estimate this counting rate. The results so obtained are shown in Table 33.

Calibration and "unknown" counts were also made in the coincidence mode, but analysis of these data has not been completed.

CONCLUSION

While these measurements do not cover a sufficiently large range of conditions to be conclusive, the agreement (of the order of 5%) between the amount of activity known to have been incorporated into the "unknown" and that calculated, as well as the consistency in depth localization, is reassuring. It suggests that calibration data utilizing a small source may be used to estimate the position and intensity of a larger, irregularly-shaped radioactive body. The use of a small, regularly-shaped source is usually more convenient from a physical standpoint, and insures that its "effective center" and geometric center coincide, i.e., that it behaves like an idealized point source.

The uncertainties introduced by lateral displacement of the "unknown liver" in the phantom were evaluated roughly, and do not appear to be significant for displacements of 4 to 6 cm at the spacing employed. In human counting, greater uncertainties may perhaps exist if the measurements are made by individuals without the requisite knowledge of normal variations in anatomy among individuals and the ability to determine organ position and orientation by palpation, auscultation or other methods of physical examination. It would seem that this limitation is not fundamental. It should be noted that radiographs were available of the Thorotrast patients counted, which revealed the spleen quite well but did not prove of great value in demonstrating the liver.

APPENDIX II

Calibration of the counting data in coincidence over the shins was accomplished by means of a leg phantom containing a known amount of ThO_2. A length of 4-mm OD Tygon tubing was loaded with the radioactive material and inserted into a hole drilled through the long axis of a human tibia. The ends were sealed with epoxy. The tibia and matching fibula were then inserted into a hollow plastic manikin leg of the type sold for the display of nylon hosiery, care being taken to approximate their anatomically-correct location. The leg was filled with water, retained by a Lucite end-plate and filling plug at the knee. Counts were made with this phantom placed in the standard human shin counting geometry illustrated in Figure 44.

The amount of Tl^{208}, principal contributor to coincidence events, which was actually present in the phantom, was then determined from an estimate of the degree of equilibration of the ThO_2 powder used. This was determined by comparison of the gamma spectrum and relative decay rate with that from an old bottle of Thorotrast, having an expiration date of 1937 and hence at least 95% equilibrated.

The leg burdens of the four individuals listed in Table 32, as corrected for lack of equilibrium of injected material (and assuming primary separation to have taken place three years prior to injection date) are as follows:

0016516

MM	0.04 g ThO_2 in equilibrium			
HR	0.07 "	"	"	
RP	0.03 "	"	"	
JJ	0.05 "	"	"	

By assuming that the portion of the skeleton viewed by our setup equals 18%,[6] and by assuming that the whole-body $Tl^{208}/Th^{232} = 0.4$ as before, we can calculate the skeletal content as:

MM 0.22 g $\simeq$ 14% of Tl^{208} body burden $\simeq$ 5.6% of Th^{232}

HR 0.39 g $\simeq$ 8% of Tl^{208} body burden $\simeq$ 3.2% of Th^{232}

RP 0.17 g $\simeq$ 12% of Tl^{208} body burden $\simeq$ 4.8% of Th^{232}

JJ 0.28 g $\simeq$ 16.5% of Tl^{208} body burden $\simeq$ 6.6% of Th^{232}.

Considering the preliminary character of these measurements, we find these figures in fair accord with measurement of skeletal samples containing marrow.[7]

It should be noted that a nonnegligible portion of the counts observed in coincidence may originate, in fact, from the Ac^{228}-Th^{228} decay. The extent of this contribution, relative to the Tl^{208}-Pb^{208} must differ for the *in vivo* and *in vitro* cases. The above data have not been corrected for this.

REFERENCES

1. L. D. Marinelli and H. F. Lucas, Jr. Translocation of Thorium Daughters to Bone. *Some Aspects of Internal Irradiation*, Proc. Symp., Heber, Utah, May 8–11, 1961. Pergamon Press, London, 1962, pp. 499–516.
2. S. Bjornholm, O. Nathan, O. B. Nielsen, and R. K. Sheline. *Nucl. Phys.* **4**, 313–324 (1957).
3. R. Chase. *Rev. Sci. Instr.* **31**, 945–949 (1960).
4. D. E. A. Jones and H. C. Raine. *Brit. J. Radiol.* **34**, 510 (1961).
5. R. Thoraeus. *Acta Radiol.* (Therapy, Physics, Biology) **3**, 81–86 (1965).
6. F. W. Spiers and P. R. J. Burch. *Brit. J. Radiol. Suppl. No. 7*, 88 (1957).
7. L. D. Marinelli and H. F. Lucas, Jr. *Argonne National Laboratory Radiological Physics Division Semiannual Report*, January through June 1962. ANL-6646, p. 95.

GAMMA-RAY BACKGROUNDS IN THE RPY VAULT: STABILITY AND RADON DEPENDENCE

J. B. Corcoran and F. Markun

The RPY low-level gamma ray counting facility (called the "vault") has been previously described.[1] It includes an iron room and other shielding devices in an underground chamber and features a controlled supply of essentially radon-free air.[2] This report describes a series of measurements to determine gamma-ray background stability in the vault under normal operating conditions and to assess the contribution radon makes to the background.

EQUIPMENT CONFIGURATION

Equipment consisted of two NaI (Tl) scintillation crystals positioned in the approximate center of the Iron Room. The smaller crystal (7″ x 3″ crystal) is 7 inches in diameter and 3 inches thick with a single 5-inch quartz photomultiplier tube. This crystal assembly has a very low intrinsic background with spectral details barely visible. The larger crystal (11″ x 4″ crystal) is 11½ inches in diameter and 4 inches thick. It has seven 3-inch glass photomultiplier tubes which contribute about 20% of the background and evidence themselves by considerable spectral detail.

The two crystals were hooked up to entirely independent electronic systems. The 11″ x 4″ was connected to a Nuclear Data 512-channel analyzer and the 7″ x 3″, a RIDL 400-channel analyzer. Individual high-voltage supplies and pre-amplifiers were also used. The two analyzers were run concurrently on 40-minute auto-repeat cycles. Daily adjustments kept the synchronization drift to less than a maximum of two minutes.

BACKGROUND STABILITY

Under normal vault conditions background stability was established by a series of 55 runs starting May 1, 1965, and extending through May 3. The radon-removal system was operating normally, maintaining the vault radon level at 0.018 ± 0.006 pCi/l. The punched paper tape output from the analyzers was processed on the CDC 160-A computer by the 1839/RPY data processing system[3] which reduced the data to counts per minute and summed the counts in nine energy bands. The sums were output from the 160-A on punched cards which were used as input to the CDC 3600 com-

0016517